Soft Matter

Accepted Manuscript

ROYAL SOCIETY OF CHEMISTRY

www.rsc.org/softmatter

CO_2 foam properties and the stabilizing mechanism of sodium bis(2-ethylhexyl)sulfosuccinate and hydrophobic nanoparticle mixtures

Chao Zhang[a], Zhaomin Li[a,*], Qian Sun[a], Peng Wang[a], Shuhua Wang[b], Wei Liu[c]

[a] College of Petroleum Engineering, China University of Petroleum, Qingdao 266580, Shandong, China

[b] Schulich School of Engineering，University of Calgary，Calgary T2N1N4，Alberta，Canada

[c] Post-Doctoral Research Center of Tarim Oilfield, Koria 841000, Xinjiang, China

Abstract: In this work, we have prepared of CO_2-in-water foam by mixing partially hydrophobic SiO_2 nanoparticles and sodium bis(2-ethylhexyl)sulfosuccinate (AOT) and studied its properties. Observation of the appearance of the foam revealed that, with the continuous addition of AOT, the phase behavior of the SiO_2 nanoparticle and AOT mixed system transformed from that of a two-phase system of aggregated nanoparticles to that of a uniform dispersed phase. Both foaming ability and foam stability were optimized when the nanoparticles and the AOT were mixed in a proportion of 1:5. On the basis of our findings from measurements of the dispersion properties, including measurements of the adsorption isotherm of the surfactant on the nanoparticles, zeta potentials, interfacial tension and the three-phase contact angle, we concluded that the synergistic interactions between the SiO_2 nanoparticles and the AOT led to the adsorption of nanoparticles around the bubble surface and the formation of a spatial network structure of nanoparticles in the film, thereby enhancing the mechanical strength of the bubble and improving the resistance to outside disturbances, deformation and drainage. Laser scanning confocal microscopy (LCSM) analysis of the same foams further confirmed the existence of a “viscoelastic shell” wrapped around and protecting the bubble.

Keywords: AOT; adsorption; carbon dioxide; foaming ability; foam stability; SiO_2 nanoparticles

1. Introduction

Enhanced oil recovery (EOR) using carbon dioxide (CO_2) as displacement agent has become a popular option in oil-and-gas field development, particularly in miscible flooding areas, where as much as 20% of the original oil could be recovered in place.[1] However, CO_2 usually flows along high-permeability zones or fractures; thus, the oil in the low-permeability zones cannot be displaced effectively.[2,3] Moreover, CO_2, as a consequence of its low density and low viscosity compared with oil and water, often rises too high in the reservoir (gravity override) or fingers unevenly, resulting in poor sweep efficiency.[4-6] The formation of foams is a promising method to increase the apparent viscosity of CO_2 in porous media by wrapping the gas into bubbles in an aqueous foam.[7-10] It has been used in site applications since the 1960s in China and has already

been developed into a series of oil-displacement techniques after more than 50 years of practical application.[11] However, foam is actually a thermodynamically unstable system.[12] Therefore, foam stability is a key factor in this application.

Recently, foams stabilized by nanoparticles have received special attention in areas such as food-making processes,[13] flotation,[14] water-borne coatings[15], and EOR.[16,17] An advantage of nanoparticles for the stabilization of foams is that they can irreversibly adsorb at CO_2/water interfaces, potentially providing greater long-term stability than traditional surfactants that dynamically adsorb and desorb at the interface.[18-20] Even more importantly, nanoparticles can be produced from chemically stable, abundant, inexpensive, and environmentally benign materials.[21-23]

Not all types of nanoparticles can stabilize CO_2-in-water foams with surfactants acting in synergy.[24] The research on the compatibility between nanoparticles and surfactants is helpful for directing the optimum use, and the hydrophilic/CO_2-philic balance (*HCB*) of the nanoparticles and surfactants is a key factor for optimization.[25-27] For instance, surfactants with low *HCB*s have been used to stabilize water-in-CO_2 (W/C) microemulsions[28-30] and emulsions,[31,32] whereas surfactants with high *HCB*s stabilize CO_2-in-water (C/W) emulsions[33,34] and foams[35].

Conventional SiO_2 nanoparticles are too hydrophilic to stabilize C/W foams; thus, surface modification via the formation of covalent bonds has been used to lower the *HCB*.[36,37] Numerous chemical agents can be used to modify nanoparticle surfaces, including CO_2-philic fluorinated ligands, hydrophobic dichlorodimethylsilane (DCDMS), amphiphilic poly(ethylene glycol) (PEG), etc.[38-41] Sodium bis(2-ethylhexyl)sulfosuccinate (AOT) is a unique anionic surfactant that contains a twin hydrocarbon tail. It has been widely used to be solubilized in super critical CO_2 (sc-CO_2) and form W/C reverse microemulsions with a certain amount of co-solvent[42,43]. Water is readily solubilized in the polar core of the reverse microemulsions to form a "water pool", which has been extensively used as a novel microreactor for carrying out many kinds of chemical and biochemical reactions[44-46]. AOT reverse microemulsions formed in sc-CO_2 are thermodynamically stable aggregates of the amphiphilic surfactant, resulting in a hydrophilic head group region surrounding a nanosized water core with hydrophobic tails extending into a non-polar continuous phase[47]. In contrast to W/C reverse microemulsions, the stable C/W foams can also be formed by AOT with a certain amount of SiO_2 nanoparticles. Here, we investigate the properties of a C/W foam prepared using partially modified SiO_2 nanoparticles and the surfactant AOT. First, the properties of SiO_2/AOT aqueous dispersions are described and discussed systematically in relation to surfactant adsorption, nanoparticle wettability and zeta potential. Then, the properties of foams prepared by SiO_2/AOT aqueous dispersions are studied, including their foaming ability and foam stability. In addition, the collaborative mechanisms of SiO_2/AOT in stabilizing a foam are discussed. We hope that this study will promote the application of nanoparticle-stabilized foams in other similar oil-related fields.

2. Experimental Section

2.1. Materials

CO_2 (99.999% purity) supplied by Tianyuan, Inc. (China) was used as received. Water was first passed through an Elga reverse-osmosis unit and then a Milli-Q reagent water system. Sodium hydroxide (96% purity) provided by Sinopharm Chemical Reagent Co., Ltd. (China) was used to adjust the aqueous-phase pH. AOT (minimum 99%, MW 444.56) purchased from Sigma Chemical

Co., Ltd. (USA) was vacuum dried at 60 °C for 24 h and stored in a vacuum desiccator prior to use. The critical micelle concentration (*cmc*) in water at 25 °C was 2.5 mM. Hydrophobic SiO_2 nanoparticles (HDK, H18, 99.8% purity) were supplied by Wacker Chemical Co., Ltd. (Germany). It is a white powder consisting of nearly spherical particles with an average diameter of approximately 12 nm. The hydrophobic SiO_2 nanoparticles were modified with DCDMS, and the silanol group density was approximately 0.5/nm^2. The specific surface area was approximately 120 m^2/g. Its weight loss was less than 0.6 wt% after being dried for two hours at 105 °C. The point of zero charge (P.Z.C.) of the hydrophobic SiO_2 nanoparticles, which was measured by the zeta-potential method, was 4.6.[48] Experiments were conducted at room temperature unless otherwise specified.

2.2. Preparation and characterization of the SiO_2/AOT aqueous dispersions

To produce well-dispersed aqueous suspensions, the SiO_2/AOT dispersions were prepared by first adding the hydrophobic SiO_2 nanoparticles into a certain concentration of AOT solution and then sonicating the resulting mixture with a 2000-W ultrasonic processor (YP-S17, 20 kHz, volume processing capacity: 0-2000 mL, Hangzhou Success Ultrasonic Equipment Co., Ltd. (China)) at an operating frequency of 20 kHz for 10 min to disperse the nanoparticles. The work-time and rest-time intervals for sonication were both set at 10 s to avoid overheating and foaming. Cold water was circulated through the container jacket using refrigerating and heating circulators (F12-EH, JULABO Labortechnik GmbH Co., Ltd. (Germany)) to maintain the temperature of the aqueous dispersions at 25 °C. The initial pH values of the SiO_2/AOT aqueous dispersions ranged from 5.58 to 6.53; the pH was adjusted to 9.8 by adding sodium hydroxide to give the particles an appreciable negative charge.

2.3. Adsorption of AOT onto the SiO_2 particles

Ten milliliters of the prepared dispersion was centrifuged (GT10-1, Beijing Shidai Beili Centrifuge Co., Ltd. (China)) at 8000 rpm for 60 min. The concentration of AOT in the supernatant was analyzed by the TOC technique. The adsorption amount was then calculated as the difference between the initial concentrations divided by the mass of the dried solid.

2.4. Stability of the SiO_2/AOT aqueous dispersions

Twenty milliliters of prepared dispersion was first transferred into a 25 mL colorimetric tube. The phase behavior of the dispersions was then observed after 1 week.

2.5. Zeta potential of SiO_2/AOT aqueous dispersions

The zeta potential of the SiO_2/AOT aqueous dispersions was measured using a Malvern Zetasizer (Nano ZS90, Malvern Instruments, Ltd., UK). The equilibrated dispersion was sonicated for 10 min and then transferred into a disposable cell for zeta-potential measurement. The cell was maintained at 25 °C for 120 s. Each sample was measured at least 5 times, and the results were averaged. The zeta potential values were calculated according to the Smoluchowski equation.[49]

2.6. Three-phase contact angle of particles

The classic captive drop method was used to measure the three-phase contact angle of the SiO_2 particles.[50] The prepared dispersion was first centrifuged (GT10-1, Beijing Shidai Beili Centrifuge

Co., Ltd. (China)) at 8000 rpm for 60 min. The lower layer was then washed with water to remove the unabsorbed AOT molecules and subsequently dried at 60 °C to yield particles. The particles were crushed into a powder that was then compressed into a circular disk. The three-phase contact angle of the disk was directly measured using a drop-shape tensiometer (Tracker-H, Teclis Co., France). Each sample was measured at least 5 times, and the results were averaged.

2.7. Properties of CO_2 foams generated from SiO_2/AOT aqueous dispersions

To produce the CO_2 foams, experiments were conducted in a fume hood that was fully filled with CO_2 at ambient pressure unless otherwise specified. CO_2 foams were first prepared using 100 mL of SiO_2/AOT aqueous dispersion and a Warning blender (GJ-3S, Qingdao Senxin Machinery Equipment Co., Ltd., China) operated at 8000 rpm for 3 min. The generated foam was immediately transferred into a glass cylinder to record the change of foam volume over time.

The properties of the CO_2 foam were also characterized using a Foamscan apparatus (Teclis Co., France). The development of the foam over time and the liquid content in the foam were observed by CCD cameras and conductivity measurements, respectively.[51,52] The foams were generated by injecting CO_2 at the required flow rate through a porous glass disc (pore diameter 0.2–0.4 μm) at the bottom of a glass tube containing 60 mL of SiO_2/AOT aqueous dispersion. Three pairs of electrodes on the inner-wall of the glass tube were used to measure the volume of the liquid. The development of the bubble size was observed by a CCD camera every 20 s. The CO_2 injection was stopped when the foam volume reached 200 mL; the evolution of the foam was then analyzed.

2.8. Interfacial tension measurements

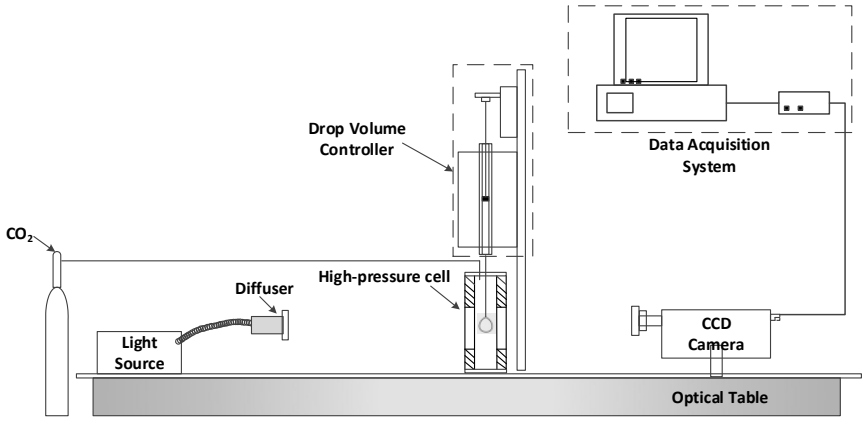

Fig. 1. Schematic of the combined pendant-droplet dynamic tensiometer and surface dilational rheometer.

The interfacial tension (*IFT*) was measured through a drop-shape tensiometer (Tracker-H, Teclis Co., France). A schematic of the instrument is shown in Fig. 1. The main parts of the instrument include a dosing system, a light source, a CCD camera, a frame grabber, a needle for drop formation and a high-pressure fixed-volume view cell consisting of a stainless steel block with two sapphire windows. Thus, the drop shape could be observed through the windows using the CCD camera. The volume of the view cell was 400 cm^3, and it could withstand a maximum pressure of 20 MPa.

Before the measurement, the view cell was fully filled with CO_2 at ambient pressure. A pendant drop of the aqueous dispersion was then formed at the end of a stainless steel needle attached to a gas-tight syringe. When a new drop formed, the drop-shape apparatus provided automatic

feedback of the drop area and drop volume during the experiments. Thus, the dynamic *IFT* was recorded through axisymmetric drop-shape analysis. Droplets of the dispersions were maintained for 10 min to reach a steady *IFT*. The dosing system, controlled by the computer, then triggered periodical oscillations at a certain frequency and a volume amplitude of 1 μm^3 and measured the corresponding changes in the *IFT*. The drop shape, drop volume and area were recorded by the CCD camera and were subsequently analyzed using commercially available drop-image software. The viscoelasticity, which was originally proposed by Gibbs, was given by

$$\varepsilon = \frac{d\gamma}{d\ln A} \tag{2}$$

where ε is the interfacial dilational viscoelasticity, γ is the interfacial tension, and A is the interfacial area. This parameter gives the interfacial resistance to changes in area or volume, which directly affects the foam stability. Details about the tensiometer and methods are available elsewhere.[53]

3. Results and Discussion

3.1. Properties of SiO_2/AOT aqueous dispersions

Because of the hydrophobic properties of the SiO_2 nanoparticles (the air-water-SiO_2 contact angle is 122°), a 2000-W ultrasonic processor was used to disperse the SiO_2 nanoparticles into AOT solutions. The effect of sonication on the SiO_2/AOT aqueous dispersions is shown in Fig. 2. The SiO_2 nanoparticles present in the conventional stirred aqueous dispersions were obviously aggregated. Under the influence of high-intensity ultrasonic cavitation, the aggregated SiO_2 nanoparticles were impacted by the surfactant-enriched water droplets of micron size because of cavitation forces. The aggregation of the nanoparticles was significantly decreased, thus providing more opportunities for the nanoparticles to contact the surfactant. Ultrasonic cavitation could be a better choice for the preparation of SiO_2/AOT aqueous dispersions.[54]

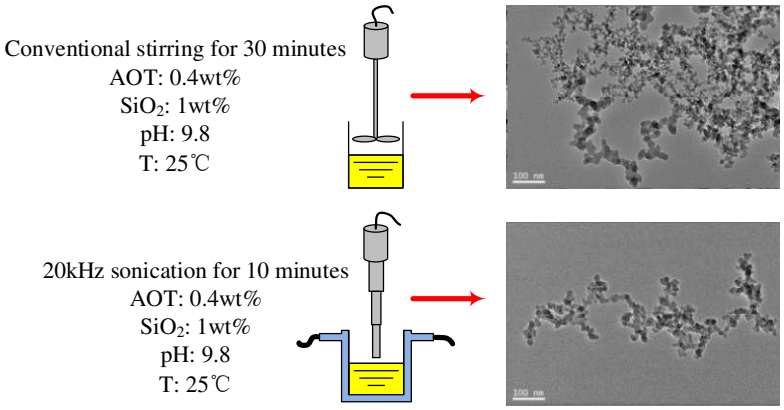

Fig. 2. TEM images of conventional stirring aqueous dispersions and ultrasound-assisted aqueous dispersions.

Because the hydrophobic SiO_2 nanoparticles were modified with dimethyl siloxane, the P.Z.C. of the hydrophobic SiO_2 nanoparticles was 4.6[48]. To induce a high particle surface charge, concentrated NaOH was subsequently added to adjust the pH of the SiO_2/AOT aqueous dispersion to 9.8. At a fixed particle concentration of 1 wt%, the addition of AOT led to a dramatic change in the stability of the aqueous dispersions. Fig. 3 illustrates that, when the AOT concentration was low, the phase separation of the dispersive system was obvious because of the hydrophobicity of the particles. As a result, the flocculated particles accumulated at the bottom of the test tube. As

the AOT concentration was increased, the sedimentation extent began to decrease and the liquid of the top layer became turbid. When the concentration was increased to 0.40 wt%, flocculent particles were dispersed completely and the dispersive system became color uniform. It is likely that the adsorption of AOT on SiO_2 nanoparticles improves their dispersion stability.

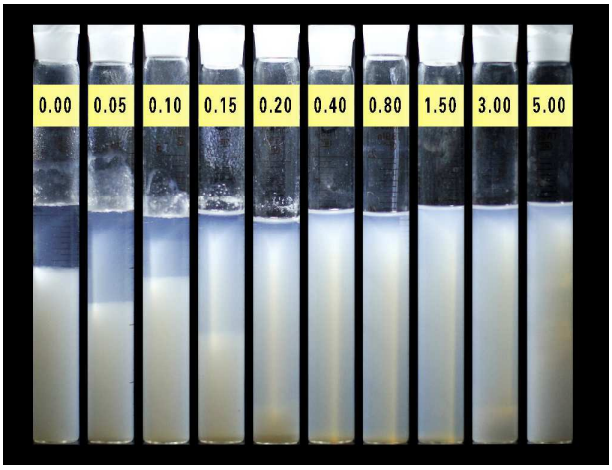

Fig. 3. Photograph of the SiO_2/AOT aqueous dispersions. (The AOT concentrations are shown in the picture (wt%); the particle concentration is fixed at 1.0 wt%.).

Zhang et al. and Binks et al. both studied the adsorption of surfactants with opposite charges onto hydrophilic particles, which have changed the dispersion properties of nanoparticles.[55,56] They demonstrated the existence of a monolayer or a bilayer of surfactants on the particle surface, where the surfactant molecules were adsorbed by electrostatic attraction. The formation of the monolayer or bilayer could change the wettability of the particles, which could also make the particles adsorb and remain at the surfaces of air bubbles, stabilizing the foam.

In order to verify the extent of AOT adsorption on hydrophobic SiO_2 nanoparticles surfaces, we have determined the adsorption isotherm using the depletion from solution method and the results are shown in Fig. 4 (a). There is a gentle increase in the adsorbed amount initially followed by a more significant increase at higher concentrations, ending close to the *cmc*, which can be described as an "S"-type isotherm with three regions. Meanwhile, because the zeta potential of nanoparticles directly reflects the adsorption of surfactant onto nanoparticles, electrophoretic measurements were performed with SiO_2 dispersions as a function of the AOT concentration, the results are presented in Fig. 4 (b). The zeta potential in the absence of surfactant is -7.12 mV at this high pH. The addition of AOT gradually decreases the potential at 0.17 mM, after which the potential significantly decreases until 5.47 mM, which can also be divided into three regions. The adsorption of AOT on the SiO_2 nanoparticles surfaces is mainly controlled by the electrostatic forces and hydrophobic interactions. In region I, the zeta potential of nanoparticles is so small (about -10 mV) that the hydrophobic attractive interaction between the twin hydrocarbon tails of AOT and the modified nonpolar groups of nanoparticles is dominant here, hence, AOT monomers adsorb individually with their polar groups extending into the bulk and decrease the zeta potential of nanoparticles. In region II, the aggregated nanoparticles start to disperse when the zeta potential of nanoparticles decreased to a certain degree. Once the aggregated nanoparticles have dispersed, which will increase the amount of available area for AOT monomers to adsorb on. Meanwhile, the polar head of the AOT will be oriented away from the surface of the nanoparticles due to electrostatic repulsion, resulting in a greater probability of the twin hydrocarbon tails contacting

the nonpolar group on the surface of the nanoparticles. As a result, there is a significant increase of the adsorption of AOT monomers on the nanoparticles surfaces and the magnitude of the potential of nanoparticles. In region III, the adsorbed amount reaches a plateau value and the nanoparticles are well dispersed.

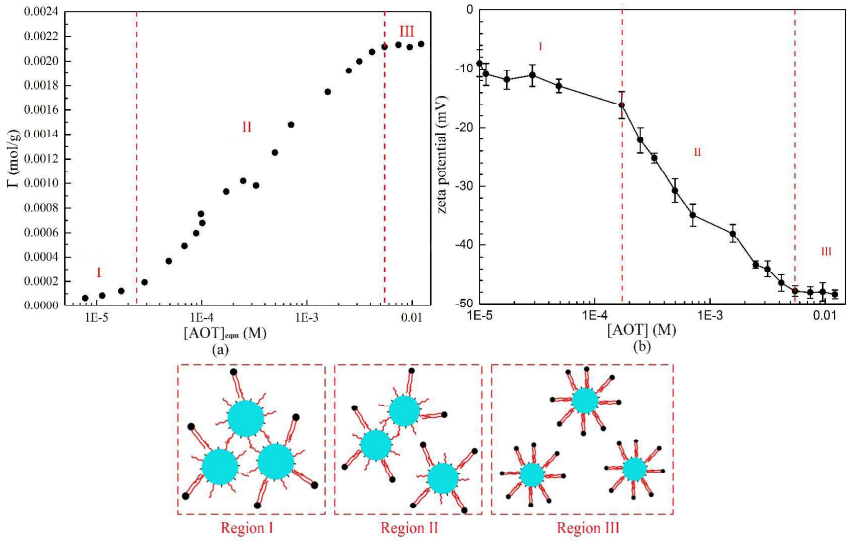

Fig. 4. Adsorption isotherm of AOT surfactant on the hydrophobic SiO_2 nanoparticles in water (a) and Zeta potential of SiO_2/AOT aqueous dispersions (b) (the SiO_2 concentration are both 1.0 wt%); pH = 9.8.

The wettability of the particles is generally described by their contact angle, which is an important piece of evidence in determining the adsorption of AOT at the particle surfaces. The variation of the three-phase contact angle values of the SiO_2 particles with increasing AOT concentration is shown in Fig. 5. In the absence of the surfactant at this high pH, the contact angle of the SiO_2 particles is 122°, indicating that the particles are hydrophobic. Increasing the AOT concentration results in a decrease in contact angle to a minimum of 73°. The SiO_2 particle surfaces thus undergo a transition from hydrophobic-to-intermediate wettability to hydrophilic wettability, which confirms that the AOT monomers are adsorbed onto the SiO_2 nanoparticles surfaces with the polar groups extending into the bulk due to the hydrophobic attractive interaction between the twin hydrocarbon tails of AOT and the modified nonpolar groups of SiO_2 nanoparticles.

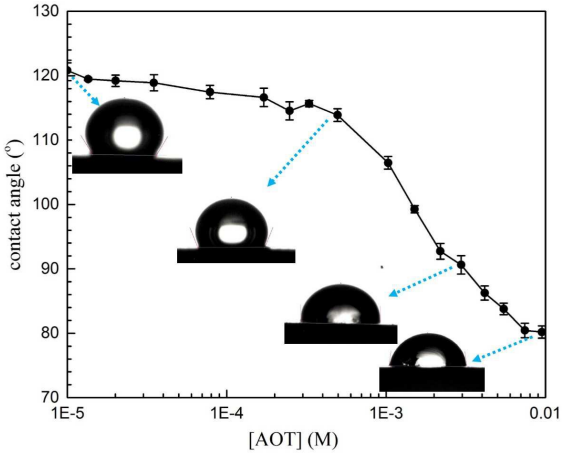

Fig. 5. Three-phase contact angle of SiO_2 particles (1.0 wt%) as a function of the AOT concentration; pH = 9.8.

3.2. Foaming ability of SiO_2/AOT aqueous dispersions

The foam volumes of the SiO_2/AOT aqueous dispersions are shown in Fig. 6. The AOT concentration in the dispersion is expressed by a relative concentration (*RC*, wt%/wt%), which refers to the ratio between the AOT concentration and the SiO_2 concentration in the dispersions, unless otherwise specified. The concentrations of SiO_2 in the dispersions investigated were 0.5, 1.0, 1.5 and 2.0 wt%, and the AOT concentrations were varied from *RC* = 0 to 1 at each nanoparticle concentration. The foam volume increased with increasing concentration of SiO_2 nanoparticles at concentrations below 1.5 wt%. A further increase of the SiO_2 concentration, however, resulted in a significant decrease of the foam volume; the foam volume of SiO_2 at 2.0 wt% was even lower than that of SiO_2 at 0.5 wt%. For each nanoparticle concentration, the foam volume increased gradually with increasing AOT concentration and reached a maximum at the same AOT/SiO_2 concentration ratio (*RC* ≈ 0.4).

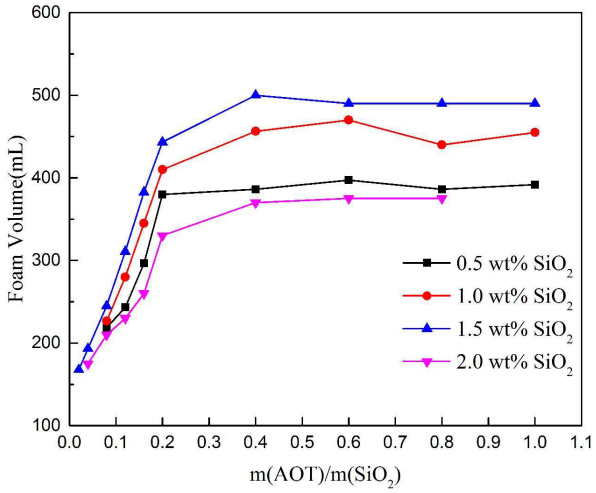

Fig. 6. Foam volume of SiO_2/AOT aqueous dispersions as a function of the relative AOT concentration (*RC*) at different SiO_2 concentrations.

To study the mechanism of the foaming ability, the *IFT* of the SiO_2/AOT aqueous dispersions with CO_2 were investigated; the results are shown in Fig. 7(a). For each nanoparticle concentration, the *IFT* value decreased gradually with increasing AOT concentration and exhibited an inflection point at the same AOT/SiO_2 concentration ratio (*RC* ≈ 0.4), which is defined as the *cmc* of AOT. The schematic illustration of the synergistic influence mechanism of SiO_2/AOT on the *IFT* is shown in Fig. 8. In region I, the concentration of AOT is lower, and the AOT monomers mainly adsorb into the CO_2/liquid surface, as a result, the amount of AOT monomers in the bulk is small. At this stage, the main factor affecting the *IFT* values is AOT monomers at the surface. Hence, the *IFT* value decreases gradually with increasing AOT concentration. In region II, there are sufficient AOT monomers to aggregate in the bulk with the continuing increases of AOT concentration. Though both AOT monomers and SiO_2 nanoparticles have the same negative charge, the hydrophobic attractive interaction between the twin hydrocarbon tails of AOT monomers and the modified nonpolar groups of nanoparticles still promote the migration of AOT monomers to adsorb onto the surface of SiO_2 nanoparticles. This phenomena has been discussed in detail for the interaction of surfactant with hydrophobically modified polymers[57, 58], which was also dependent on the hydrophobic attractive interaction. Meanwhile, the electrostatic repulsion between AOT monomers and SiO_2 nanoparticles keeps the hydrophilic head group of AOT monomer away from

SiO_2 nanoparticles surface, which promotes the contact between the hydrophobic tails of AOT monomers and SiO_2 nanoparticles. In related investigations[59-61], the effect of alcohols and urea on micelle formation has been found to increase the *cmc* due to the diminishing of the hydrophobic effect. Similarly, the adsorption of AOT monomers on SiO_2 nanoparticles will diminish the hydrophobic effect of AOT monomers in solution, that is, it would hinder the micellization of AOT monomers, leading to an increase of the *cmc* of AOT, as shown obviously in Fig. 7(a). In region III, the nanoparticle-nanoparticle electrostatic repulsion increases due to the decreased zeta potentials of nanoparticles, which will promote the dispersion of nanoparticles in the bulk, in agreement with the results in Fig. 4(b). Caused by the adsorption of AOT monomers, the polar groups are introduced into the surfaces of SiO_2 nanoparticles. It will change the wettability of parts of the dispersed SiO_2 nanoparticles from hydrophobic to amphiphilic: the nonpolar group on the surface of the nanoparticles adsorbed with AOT monomers shows hydrophilic, whereas the nonpolar group without adsorption of AOT monomers still shows hydrophobic. Therefore, the dispersed nanoparticles shows a tendency to adsorb upon the CO_2/liquid surface because of the hydrophobicity[62,63], and the *IFT* value are still decreasing because of the surface active. Meanwhile, the AOT monomers will bend towards to the liquid to ensure that the polar group will extend into the liquid. Only in this way can the nanoparticles adsorbed on the CO_2/liquid surface with low interfacial energy. In region IV, with the continuing increases of AOT concentration, AOT monomers dispersed in the bulk tend to adsorb onto the surface of the other parts of the dispersed SiO_2 nanoparticles, which will cause these nanoparticles to be hydrophilic rather than amphiphilic, and hinder the migration of these nanoparticles to adsorb on the CO_2/liquid surface. Then, the *IFT* reaches a plateau value. It can also be seen that the *IFT* values of the SiO_2/AOT aqueous dispersions decrease with increasing SiO_2 concentrations, whereas the SiO_2 concentration at 2.0 wt% is just slightly lower than the *IFT* of the SiO_2 concentration at 1.5 wt%. It indicates that the more SiO_2 nanoparticles introduced, the more advantageous for the formation of amphiphilic particles. However, when the CO_2/liquid surface contains the maximum number of the amphiphilic particles allowed, AOT monomers will be adsorbed at the surface of the excess amphiphilic particles, induce the transformation of these nanoparticles from amphiphilic to hydrophilic, which will facilitate the stable dispersion of these nanoparticles in the bulk, but do not affect the *IFT* values of the SiO_2/AOT aqueous dispersions.

The above situations indicate that a synergistic effect occurs between the nanoparticles and the AOT to reduce the *IFT* values of the SiO_2/AOT aqueous dispersions, which implies that the formation of foam requires less energy, thus improving the foaming ability. Moreover, as shown by Xu et al.[64], the lower *IFT* can reduce the probability of foam rupture and create more successful foaming. Thus, the addition of SiO_2 nanoparticles to the AOT solution can facilitate the formation of a protective film at the CO_2/dispersion surface and promote the formation of foam.

It can also be seen that a significant decrease in the foam volume was observed when the concentration of SiO_2 nanoparticles was increased from 1.5 wt% to 2.0 wt%, whereas the *IFT* at an SiO_2 concentration of 2.0 wt% was only slightly lower than that at 1.5 wt%. This scenario was corroborated by viscosity measurements of the SiO_2/AOT aqueous dispersions. As reported by Zhang et al.[65], dispersions with increased viscosity require greater energy to produce a foam. Fig. 7(b) highlights the influence of the SiO_2 and AOT concentrations on the viscosity of the dispersions. The viscosity significantly increased when the concentration of SiO_2 nanoparticles was increased from 1.5 wt% to 2.0 wt%, whereas the viscosity only slightly increased when the

concentration of SiO_2 nanoparticles was increased below 1.5 wt%. Therefore, these two factors both influence the foaming ability. When the change in viscosity is small, the *IFT* of the SiO_2/AOT aqueous dispersions with CO_2 is dominant; in contrast, the viscosity is dominant when the viscosity changes significantly.

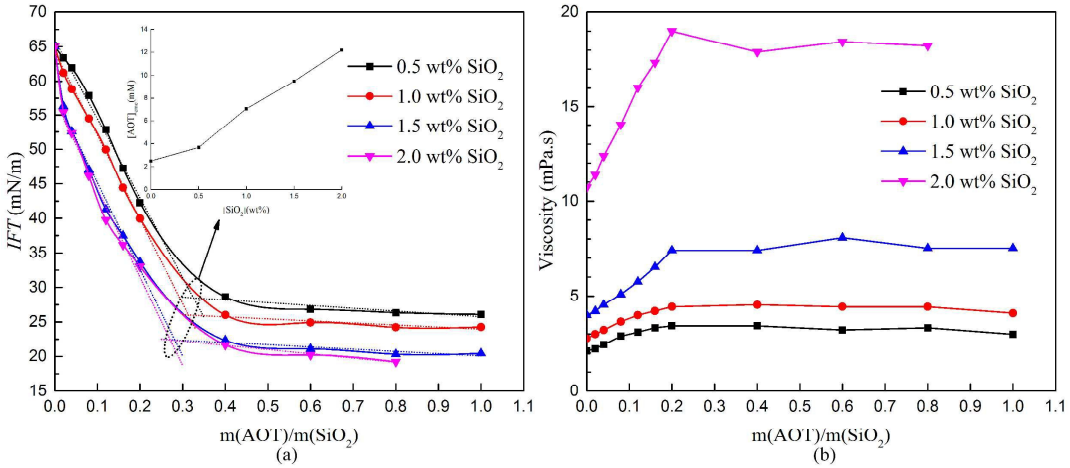

Fig. 7. The *IFT* of SiO_2/AOT aqueous dispersions with CO_2 (a) (Insert: the *cmc* of AOT at different SiO_2 concentrations) and the viscosity of SiO_2/AOT aqueous dispersions (b) as a function of the relative AOT concentration (*RC*) at different SiO_2 concentrations.

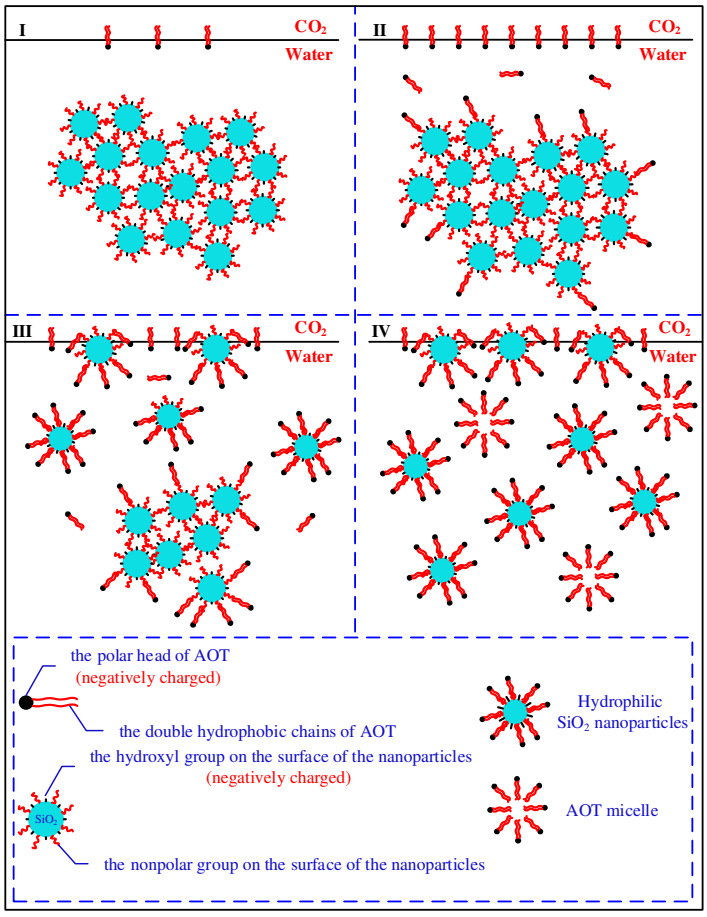

Fig. 8. The schematic illustration of the synergistic influence mechanism of SiO_2/AOT on the *IFT* .

3.3. Foam stability of SiO_2/AOT aqueous dispersions

The stability of the foams in the SiO_2/AOT dispersions was also observed to vary with nanoparticle concentration and surfactant concentration. As illustrated in Fig. 9, the most stable foams of each nanoparticle concentration were all formed at the same concentration ratio of AOT to SiO_2 (i.e., $RC \approx 0.2$). As shown in the three-phase contact-angle plot in Fig. 5, this value corresponds to nanoparticles of intermediate wettability with the contact angle nearest to 90°. The nanoparticles can adsorb onto interfaces (water-CO_2) with a suitable contact angle θ between the nanoparticle and the interface[66]: If θ measured into the aqueous phase is normally < 90°, then a larger fraction of the nanoparticle resides in the water than in the CO_2. Conversely, the nanoparticles reside more in the CO_2 than in the water when θ > 90°. Accordingly, the ratio of surfactant adsorption onto the nanoparticles is optimal when θ =s 90°, resulting in the optimal surface activity of the SiO_2 nanoparticles coated with AOT (Fig. 7 (a)). The adsorption of partially coated nanoparticles onto air-bubble surfaces may be responsible for this optimal activity. Moreover, some researchers[66] also reported that the relevant parameter of foam stability is the desorption energy *E*, which is the energy required to remove the nanoparticle from the interface and is given by

$$E = \pi R^2 \gamma_{\alpha\beta}(1 - |\cos\theta|)^2 \quad (1)$$

where R and $\gamma_{\alpha\beta}$ are the radius of the nanoparticles and the *IFT* of gas and water, respectively.

Eq. (1) shows that the nanoparticle is most strongly held at the interface when θ = 90°, which maximizes *E*.[67] The particles adsorb around the bubble surfaces, which form the nanosized particulate films; the particles can thus inhibit the coalescence, disproportionation, and film drainage. Consequently, the stability of the foam is improved.

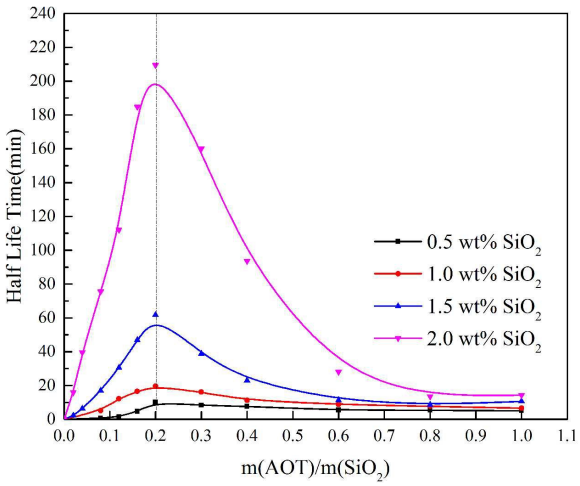

Fig. 9. Half-life of foams stabilized by the SiO_2/AOT system as a function of the relative AOT concentration (*RC*) at different particle concentrations indicated in the legend (wt%).

To confirm the adsorption of the nanoparticles around bubbles, we developed the technique of studying freshly prepared foams using SiO_2/AOT aqueous dispersions with laser scanning confocal microscopy (LSCM, Olympus Fluoview 500, Japan), as shown in Figs. 10(a) and (b). The concentrations of AOT and nanoparticles were fixed at 0.2 wt% and 1.0 wt%, respectively. The SiO_2 nanoparticles were first labeled with fluorescein isothiocyanate (FITC), and the

dispersion was subsequently washed with deionized water to remove the free FITC in the bulk. In order to observe the nanoparticles adsorbing on the bubble surface and dispersing in the bulk, we refocused LSCM on bubbles and bulk respectively, and superimposed the bright field image and fluorescence image under blue exciting light (Fig. 10). It can be observed that there are the adsorption of SiO_2 nanoparticles on the bubble surface (Fig. 10(a)) and the dispersion of SiO_2 nanoparticles in the bulk (Fig. 10(b)) at the appropriate concentrations of the nanoparticles and AOT, in conformity with the results in Fig. 8. The viscoelastic shell formed by the SiO_2 nanoparticles around the bubble surface exhibits enhanced mechanical strength to resist disturbances and deformation of the bubble[13]. Meanwhile, the formation of a spatial network structure of SiO_2 nanoparticles dispersed in the foam film strengthens the ability of the film to withstand disturbances and drainage (Fig. 10(c)). Therefore, the stabilization of foams is facilitated.

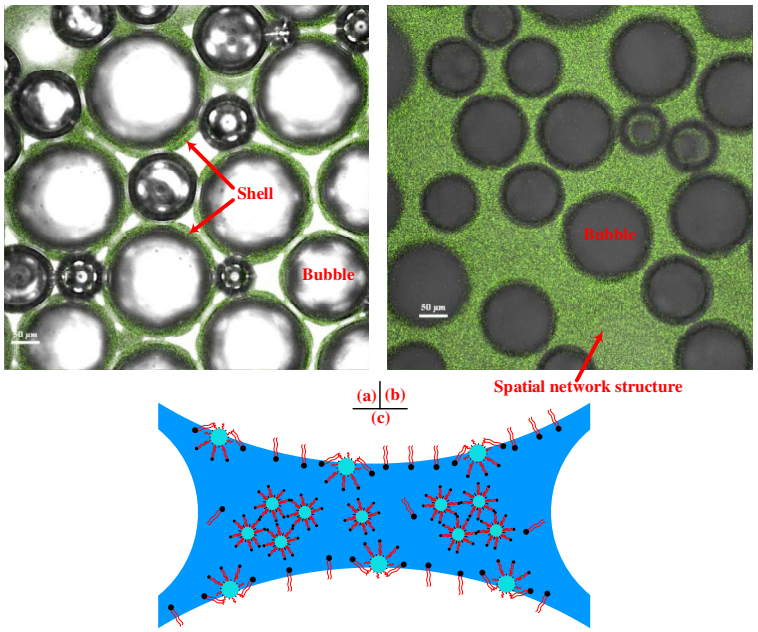

Fig. 10. Confocal fluorescence image of foams prepared with SiO_2/AOT aqueous dispersions, refocusing on bubbles (a) and bulk (b), (c) is the schematic illustration of the stabilization mechanism of SiO_2/AOT aqueous dispersions on the CO_2 foam film. (The AOT concentration is 0.2 wt%, and the nanoparticle concentration is fixed at 1.0 wt%.)

Fig. 11(a) shows a photograph of dried foams; these photographs were taken 24 h after the samples were prepared. The drained liquids became more opaque with increasing AOT concentration, which indicated that the nanoparticles changed from hydrophobic to intermediate wettability and then to hydrophilic wettability, in agreement with the results in Fig. 5. Meanwhile, the concentration of nanoparticles located in the dried foam phase decreased with increasing AOT concentration, and no dried foam residue was observed when the AOT concentration exceeded 0.2 wt%. This result indicates that the nanoparticles indeed played a role in stabilizing the foams at the proper AOT concentration by forming a three-dimensional network structure, as shown in Fig. 11(b). The existence of this spatial network gives the bubble structure its own "skeleton," which enhances the mechanical strength of the bubble and also improves the resistance to outside disturbances. As a result, the stability of the bubbles is greatly improved.

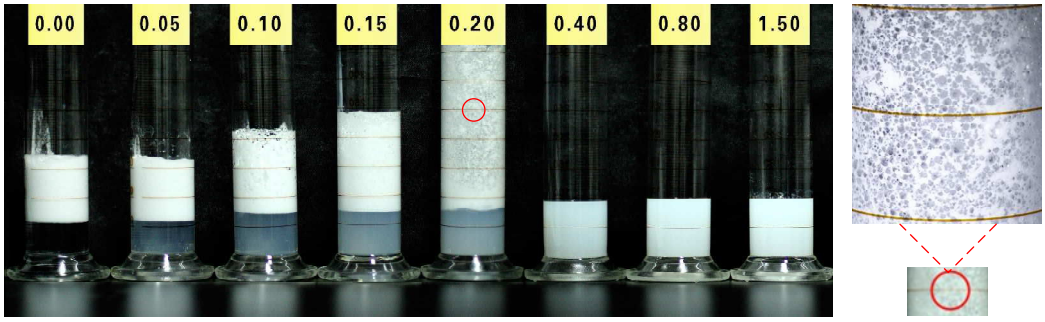

(a) (b)

Fig. 11. Photograph of dried foams prepared with SiO_2/AOT aqueous dispersions (a) and magnification of the red-circled area (b). (The AOT concentrations are shown in the picture (wt%). The nanoparticle concentration is fixed at 1.0 wt%.)

The morphology was studied with the Foamscan apparatus to confirm that the SiO_2 nanoparticles affect the foam stability with the AOT. Fig. 12 shows the morphology of a conventional aqueous foam and a SiO_2/AOT-dispersion-enhanced foam. The results show that a conventional aqueous foam with surfactant exhibits obvious inhomogeneity, with different sizes of bubbles that will easily merge into larger bubbles and finally form a single large bubble. Meanwhile, the film of the large bubble is very thin and can be easily ruptured, resulting in instability of the foam system. However, the foam becomes compact and uniform with the addition of the SiO_2 nanoparticles. The SiO_2 nanoparticles can form a viscoelastic shell around the bubble surface with AOT, as shown in Fig. 10. The viscoelastic shell can make the foam film become thicker and protect bubbles against shrinkage and coalescence.[14] As a result, the SiO_2/AOT dispersions enhance the foam stability.

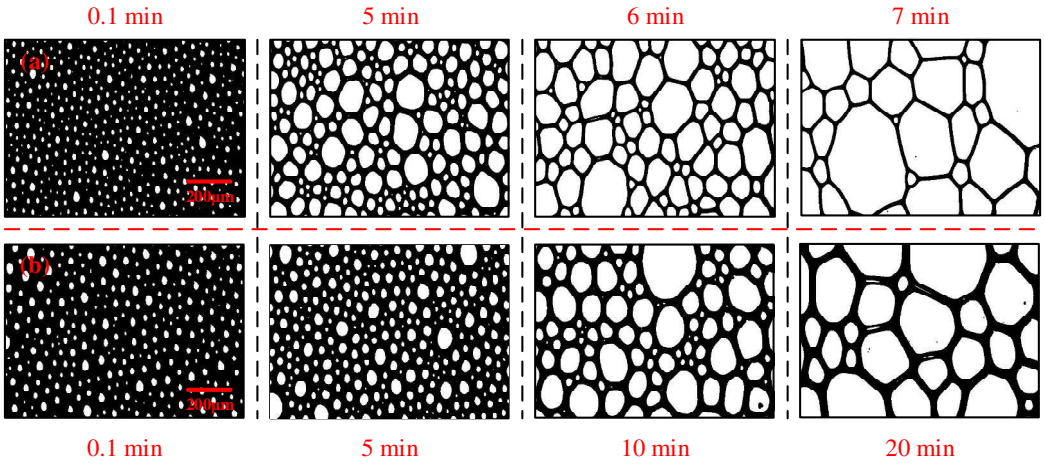

Fig. 12. Morphology of a conventional aqueous foam and a SiO_2/AOT-dispersion-enhanced foam. (a) Conventional aqueous foam with 0.2 wt% surfactant. (b) SiO_2/AOT dispersions enhanced foam (0.2wt% surfactant +1.0 wt% SiO_2 nanoparticles).

4. Conclusions

A detailed investigation into the behavior of CO_2-in-water foams stabilized by a mixture of SiO_2 nanoparticles and AOT surfactant at high pH was conducted. A synergistic effect was demonstrated to occur through the combination of both increasing the foaming ability and

improving the foam stability. When both SiO_2 nanoparticles and AOT surfactant are mixed to prepare the foam, control of the quantities of the two species is important. Interfacial tension isotherms showed that the optimal ratio between the AOT concentration and the SiO_2 nanoparticle concentration contributed to improving the effective content of surfactants at the CO_2/liquid interface to achieve the best surface activity. The wettability of the nanoparticles was adjusted via the AOT concentration because of the hydrophobic attractive interactions; thus, an optimum ratio was selected to obtain a maximum desorption energy, which enhanced foam stability. A confocal laser-induced fluorescence detection technique revealed that the nanoparticles form a viscoelastic shell wrapped around the bubbles. This shell enhances the mechanical strength of the bubbles and improves its resistance to outside disturbances. The spatial network structure of SiO_2 nanoparticles dispersed in the foam film strengthen the ability of the film to withstand disturbances, bubble deformation and drainage.

Author Information

Corresponding Author:

*Zhaomin Li. E-mail: lizhm@upc.edu.cn

Notes

The authors declare no competing financial interest.

Acknowledgments

This work was financially supported by the National Program on Key Basic Research Project (2015CB250904), National Natural Science Foundation of China (51274288), National Natural Science Foundation of Shandong Province (2012ZRE28014), National Natural Science Foundation of China- Petrochemical Industry Fund (U1262102), the Fundamental Research Funds for the Central Universities (14CX06085A), and the Special Research Fund for the Doctoral Program of High Education (20120133110008). We sincerely thank our other colleagues at the Foam Fluid Research Center at the China University of Petroleum (East China) for assisting with the experiments.

References

[1] Ren G, Zhang H, Nguyen Q. Effect of surfactant partitioning on mobility control during carbon-dioxide flooding. SPE Journal, 2013, 18(04): 752-765.

[2] W. Y. Xie, X. G. Li and Z. Y. Chen, Review of exploration and development technologies for heavy oil and high pour-point oil in Liaohe oil region, Acta Pet. Sin., 2007, 28, 145-150.

[3] Y. C. Xin, X. Y. Dong and J. P. Bian, Affecting factors for flow ability of high-salinity heavy oil and methods for improving oil mobility, Acta Pet. Sin., 2010, 31, 480-485.

[4] Rossen W R, Gauglitz P A. Percolation theory of creation and mobilization of foams in porous media. AIChE Journal, 1990, 36(8): 1176-1188.

[5] Q. T. Yu, A study on strategy and approach on enhanced ultimate recovery from oilfields, Acta Pet. Sin., 1996, 17, 35-37.

[6] Rossen W R. Foams in enhanced oil recovery. Surfactant Science Series, 1996: 413-464.

[7] R. Gharbi, E. Peters and A. Elkamel, Scaling miscible fluid displacement in porous media, Energy Fules, 1998, 12, 801-811.

[8] J. S. Kim, Y. Dong and W. R. Rossen, Steady-state flow behavior of CO_2 foam, SPE Journal, 2004, 10, 405-415.

[9] J. Zuta, I. Fjelde and R. Berenblyum, Experimental and simulation of CO_2-foam flooding in fractured chalk rock at reservoir conditions: Effect of mode of injection on oil recovery, SPE 129575, in SPE EOR Conference at Oil & Gas West Asia held in Muscat, Oman, 2010.

[10] A. A. Aleidan, D. D. Mamora and D. S. Schechter, Experimental and numerical simulation studies of different modes of CO_2 injection in fracture carbonate cores, SPE 143512, in SPE Enhanced Oil Recovery Conference held in Kuala Lumpur, Malaysia, 2011.

[11] X. S. Zhang, Q. W. Wang, X. W. Song, G. H. Zhong, P. Guo and X. L. Li, Polymer enhanced nitrogen foam injection for EOR in well group GD2-28-8 of Gudao, Shengli: Laboratory study and preliminary results, Oilfield Chemistry, 2005, 22, 366-369.

[12] Bergeron V. Disjoining pressures and film stability of alkyltrimethylammonium bromide foam films. Langmuir, 1997, 13(13): 3474-3482.

[13]E. Dickinson, Food emulsions and foams: stabilization by particles, Curr. Opin. Colloid Interface Sci., 2010, 15, 40-49.

[14] T. N. Hunter, R. J. Pugh, G. V. Franks and G. J. Jameson, The role of particles in stabilising foams and emulsions, Adv. Colloid Interface Sci., 2008, 137, 57-81.

[15] P. N. Garrett, S. P. Wicks and E. Fowles, The effect of high volume fractions of latex particles on foaming and antifoam action in surfactant solutions, Colloids Surf. A, 2006, 382, 307-328.

[16] Q. Sun, Z.M. Li, S.Y. Li, L. Jiang, J.Q. Wang, P. Wang, Utilization of surfactant-stabilized foam for enhanced oil recovery by adding nanoparticles, Energy Fuels 28 (2014) 2384-2394.

[17] J.J. Yu, M. Khalil, N. Liu, R. Lee, Effect of particle hydrophobicity on CO_2 foam generation and foam flow behavior in porous media, Fuel 126 (2014) 104-108.

[18] Johnston K P, da Rocha S R P. Colloids in supercritical fluids over the last 20 years and future directions. The Journal of Supercritical Fluids, 2009, 47(3): 523-530.

[19] Golomb D, Barry E, Ryan D, et al. Macroemulsions of liquid and supercritical CO_2-in-water and water-in-liquid CO_2 stabilized by fine particles. Industrial & engineering chemistry research, 2006, 45(8): 2728-2733.

[20] Okada M, Maeda H, Fujii S, et al. Formation of Pickering emulsions stabilized via interaction between nanoparticles dispersed in aqueous phase and polymer end groups dissolved in oil phase. Langmuir, 2012, 28(25): 9405-9412.

[21] Aveyard R, Binks B P, Clint J H. Emulsions stabilised solely by colloidal particles. Advances in Colloid and Interface Science, 2003, 100: 503-546.

[22] Studart A R, Gonzenbach U T, Tervoort E, et al. Processing routes to macroporous ceramics: a review[J]. Journal of the American Ceramic Society, 2006, 89(6): 1771-1789.

[23] Grzelczak M, Vermant J, Furst E M, et al. Directed self-assembly of nanoparticles[J]. ACS nano, 2010, 4(7): 3591-3605.

[24] Worthen A J, Bryant S L, Huh C, et al. Carbon dioxide‐in‐water foams stabilized with nanoparticles and surfactant acting in synergy. AIChE Journal, 2013, 59(9): 3490-3501.

[25] Crespy D, Landfester K. Making dry fertile: a practical tour of non-aqueous emulsions and miniemulsions, their preparation and some applications. Soft Matter, 2011, 7(23): 11054-11064.

[26] Marre S, Roig Y, Aymonier C. Supercritical microfluidics: Opportunities in flow-through chemistry and materials science. The Journal of Supercritical Fluids, 2012, 66: 251-264.

[27] Sanli D, Bozbag S E, Erkey C. Synthesis of nanostructured materials using supercritical CO_2: Part I. Physical transformations. Journal of Materials Science, 2012, 47(7): 2995-3025.

[28] Lee C T, Psathas P A, Ziegler K J, et al. Formation of water-in-carbon dioxide microemulsions with a cationic surfactant: a small-angle neutron scattering study. The Journal of Physical Chemistry B, 2000, 104(47): 11094-11102.

[29] Eastoe J, Paul A, Downer A, et al. Effects of fluorocarbon surfactant chain structure on stability of water-in-carbon dioxide microemulsions. Links between aqueous surface tension and microemulsion stability. Langmuir, 2002, 18(8): 3014-3017.

[30] Eastoe J, Gold S, Steytler D C. Surfactants for CO_2. Langmuir, 2006, 22(24): 9832-9842.

[31] Lee CT Jr, Psathas PA, Johnston KP, DeGrazia J, Randolph TW.Water-in-carbon dioxide emulsions: formation and stability. Langmuir. 1999;15(20):6781–6791.

[32] Johnston KP, Cho D, da Rocha SRP, Psathas PA, Ryoo W, Webber SE, Eastoe J, Dupont A, Steytler DC. Water in carbon dioxide macroemulsions and miniemulsions with a hydrocarbon surfactant. Langmuir. 2001;17:7191–7193.

[33] da Rocha S R P, Dickson J, Cho D, et al. Stubby surfactants for stabilization of water and CO_2 emulsions: Trisiloxanes. Langmuir, 2003, 19(8): 3114-3120.

[34] Xing D, Wei B, Trickett K, Mohamed A, Eastoe J, Soong Y, Enick RM. CO_2-soluble surfactants for improved mobility control. In: SPE 129907, Presented at SPE Improved Oil Recovery Symposium, April 24–28, 2010, Tulsa, OK.

[35] Adkins S S, Chen X, Chan I, et al. Morphology and stability of CO_2-in-water foams with nonionic hydrocarbon surfactants. Langmuir, 2010, 26(8): 5335-5348.

[36] Worthen A J, Bagaria H G, Chen Y, et al. Nanoparticle-stabilized carbon dioxide-in-water foams with fine texture. Journal of colloid and interface science, 2013, 391: 142-151.

[37] Nguyen P, Fadaei H, Sinton D. Pore-Scale Assessment of Nanoparticle-Stabilized CO_2 Foam for Enhanced Oil Recovery. Energy & Fuels, 2014, 28(10): 6221-6227.

[38] Yoon K Y, An S J, Chen Y, et al. Graphene oxide nanoplatelet dispersions in concentrated NaCl and stabilization of oil/water emulsions. Journal of colloid and interface science, 2013, 403: 1-6.

[39] Dickson J L, Binks B P, Johnston K P. Stabilization of carbon dioxide-in-water emulsions with silica nanoparticles. Langmuir, 2004, 20(19): 7976-7983.

[40] Kim Y, Wan J, Kneafsey T J, et al. Dewetting of silica surfaces upon reactions with supercritical CO_2 and brine: pore-scale studies in micromodels. Environmental science & technology, 2012, 46(7): 4228-4235.

[41] Aveyard R, Binks B P, Clint J H. Emulsions stabilised solely by colloidal particles. Advances in Colloid and Interface Science, 2003, 100: 503-546.

[42] Hutton B H, Perera J M, Grieser F, et al. Investigation of AOT reverse microemulsions in supercritical carbon dioxide. Colloids and surfaces A: Physicochemical and engineering aspects, 1999, 146(1): 227-241.

[43] M. Ji, X.Y. Chen, C.M. Wai, J.L. Fulton, Synthesizing and dispersing silver nanoparticles in a water-in-supercritical carbon dioxide microemulsion, J. Am. Chem. Soc. 121 (1999) 2631.

[44] Holmes J D, Bhargava P A, Korgel B A, et al. Synthesis of cadmium sulfide Q particles in water-in-CO_2 microemulsions. Langmuir, 1999, 15(20): 6613-6615.

[45] Ji M, Chen X, Wai C M, et al. Synthesizing and dispersing silver nanoparticles in a water-in-supercritical carbon dioxide microemulsion. Journal of the American Chemical

Society, 1999, 121(11): 2631-2632.

[46] Ohde H, Wai C M, Kim H, et al. Hydrogenation of olefins in supercritical CO_2 catalyzed by palladium nanoparticles in a water-in-CO_2 microemulsion. Journal of the American Chemical Society, 2002, 124(17): 4540-4541.

[47] Liu J, Shervani Z, Raveendran P, et al. Micellization of sodium bis(2-ethylhexyl) sulfosuccinate in supercritical CO_2 with fluorinated co-surfactant and its solubilization of hydrophilic species. The Journal of supercritical fluids, 2005, 33(2): 121-130.

[48] Pierre A. C. Introduction to sol-gel processing. Springer Science & Business Media, 1998.

[49] Sze A, Erickson D, Ren L, et al. Zeta-potential measurement using the Smoluchowski equation and the slope of the current–time relationship in electroosmotic flow. Journal of colloid and interface science, 2003, 261(2): 402-410.

[50] Yan N, Masliyah J H. Effect of pH on adsorption and desorption of clay particles at oil–water interface. Journal of colloid and interface science, 1996, 181(1): 20-27.

[51] M.J. Martine, V.M.P. Ruiz-Henestrosa, C.C. Sánchez, J.M.R. Patino, A.M.R. Pilosof, Interfacial and foaming interactions between casein glycomacropeptide (CMP) and propylene glycol alginate, Colloids Surf. B 95 (2012) 214-221.

[52] J. Boos, W. Drenckhan, C. Stubenrauch, Protocol for studying aqueous foams stabilized by surfactant mixtures, J. Surf. Deterg. 16 (2013) 1-12.

[53] X.L. Cao, Y. Li, S.X. Jiang, H.Q. Sun, A. Cagna, L.X. Dou, A study of dilational rheological properties of polymers at interfaces, J. Colloid Interface Sci. 270 (2004) 295-298.

[54] Abbas S, Karangwa E, Bashari M, et al. Fabrication of polymeric nanocapsules from curcumin-loaded nanoemulsion templates by self-assembly. Ultrasonics sonochemistry, 2015, 23: 81-92.

[55] Zhang S, Lan Q, Liu Q, et al. Aqueous foams stabilized by Laponite and CTAB. Colloids and Surfaces A: Physicochemical and Engineering Aspects, 2008, 317(1): 406-413.

[56] Binks B P, Kirkland M, Rodrigues J A. Origin of stabilisation of aqueous foams in nanoparticle–surfactant mixtures. Soft Matter, 2008, 4(12): 2373-2382.

[57] Panmai S, Prud'homme R K, Peiffer D G, et al. Interactions between hydrophobically modified polymers and surfactants: a fluorescence study. Langmuir, 2002, 18(10): 3860-3864.

[58] Wang X, Li Y, Wang J, et al. Interactions of cationic gemini surfactants with hydrophobically modified poly (acrylamides) studied by fluorescence and microcalorimetry. The Journal of Physical Chemistry B, 2005, 109(26): 12850-12855.

[59] Tanford C. The Hydrophobic Effect: Formation of Micelles and Biological Membranes 2d Ed. J. Wiley., 1980.

[60] Singh H N, Swarup S. Effect of monohydroxy alcohols and urea on the cmc of surfactants. Bulletin of the Chemical Society of Japan, 1978, 51(5): 1534-1538.

[61] Huang C C, Hohn K L. Tetrakis (dimethylamino) ethylene chemiluminescence (TDE CL) characterization of the CMC and the viscosity of reversed microemulsions. The Journal of Physical Chemistry B, 2010, 114(8): 2685-2694.

[62] Abdel-Fattah A I, El-Genk M S. On colloidal particle sorption onto a stagnant air–water interface. Advances in colloid and interface science, 1998, 78(3): 237-266.

[63] Abdel-Fattah A I, El-Genk M S. Sorption of hydrophobic, negatively charged microspheres onto a stagnant air/water interface. Journal of colloid and interface science, 1998, 202(2): 417-429.

[64] Xu L, Xu G, Gong H, et al. Foam properties and stabilizing mechanism of sodium fatty alcohol polyoxyethylene ether sulfate-welan gum composite systems. Colloids and Surfaces A: Physicochemical and Engineering Aspects, 2014, 456: 176-183.

[65] Zhang S, Sun D, Dong X, et al. Aqueous foams stabilized with particles and nonionic surfactants. Colloids and Surfaces A: Physicochemical and Engineering Aspects, 2008, 324(1): 1-8.

[66] Binks B P. Particles as surfactants—similarities and differences. Current Opinion in Colloid & Interface Science, 2002, 7(1): 21-41.

[67] Binks B P, Lumsdon S O. Influence of particle wettability on the type and stability of surfactant-free emulsions. Langmuir, 2000, 16(23): 8622-8631.